The Journal of Experimental Biology 213, 3894-3905

doi:10.1242/jeb.046870

Differential adjustment in gill Na^+/K^+- and V-ATPase activities and transporter mRNA expression during osmoregulatory acclimation in the cinnamon shrimp *Macrobrachium amazonicum* (Decapoda, Palaemonidae)

Rogério Oliveira Faleiros[1], Maria Helena S. Goldman[1], Rosa P. M. Furriel[2] and John Campbell McNamara[1,*]

[1]Departamento de Biologia, Faculdade de Filosofia, Ciências e Letras de Ribeirão Preto, Universidade de São Paulo, Ribeirão Preto 14040-901 SP, Brazil and [2]Departamento de Química, Faculdade de Filosofia, Ciências e Letras de Ribeirão Preto, Universidade de São Paulo, Ribeirão Preto 14040-901 SP, Brazil

*Author for correspondence (mcnamara@ffclrp.usp.br)

Accepted 19 August 2010

SUMMARY

We evaluate osmotic and chloride (Cl^-) regulatory capability in the diadromous shrimp *Macrobrachium amazonicum*, and the accompanying alterations in hemolymph osmolality and [Cl^-], gill Na^+/K^+-ATPase activity, and expression of gill Na^+/K^+-ATPase α-subunit and V-ATPase B subunit mRNA during salinity (S) acclimation. We also characterize V-ATPase kinetics and the organization of transport-related membrane systems in the gill epithelium. *Macrobrachium amazonicum* strongly hyper-regulates hemolymph osmolality and [Cl^-] in freshwater and in salinities up to 25‰ S. During a 10-day acclimation period to 25‰ S, hemolymph became isosmotic and hypo-chloremic after 5 days, [Cl^-] alone remaining hyporegulated thereafter. Gill Na^+/K^+-ATPase α-subunit mRNA expression increased 6.5 times initial values after 1 h, then decreased to 3 to 4 times initial values by 24 h and to 1.5 times initial values after 10 days at 25‰ S. This increased expression was accompanied by a sharp decrease at 5 h then recovery of initial Na^+/K^+-ATPase activity within 24 h, declining again after 5 days, which suggests transient Cl^- secretion. V-ATPase B-subunit mRNA expression increased 1.5-fold within 1 h, then reduced sharply to 0.3 times initial values by 5 h, and remained unchanged for the remainder of the 10-day period. V-ATPase activity dropped sharply and was negligible after a 10-day acclimation period to 21‰ S, revealing a marked downregulation of ion uptake mechanisms. The gill epithelium consists of thick, apical pillar cell flanges, the perikarya of which are coupled to an intralamellar septum. These two cell types respectively exhibit extensive apical evaginations and deep membrane invaginations, both of which are associated with numerous mitochondria, characterizing an ion transporting epithelium. These changes in Na^+/K^+- and V-ATPase activities and in mRNA expression during salinity acclimation appear to underpin ion uptake and Cl^- secretion by the palaemonid shrimp gill.

Key words: Na^+/K^+-ATPase, V-ATPase, mRNA expression, enzyme activity, ion transporters, osmoregulation, salinity acclimation, gill epithelial ultrastructure, *Macrobrachium*, palaemonid shrimp.

INTRODUCTION

Salt content is one of the most important environmental variables in any aquatic habitat, and the ability of crustaceans to survive and reproduce in media of different salinities depends on their behavioral, morphological, physiological and biochemical adaptations (Anger, 1995). Among these, osmoregulation, a process centered on active ion transport, is the most vital (Berger and Kharazova, 1997). The antennal glands and gills constitute the principal organs responsible for homeostasis of the extracellular fluid in the Crustacea (Taylor and Taylor, 1992; Péqueux, 1995; Freire et al., 2008a), and the gill lamellae provide an amplified surface area of differentially permeable interface employed in both gas and ion exchange between the internal and external media. The polarized epithelial cells or 'ionocytes' that constitute the lamellar epithelia play a key role in these ion transport processes and, in the gills of strongly osmoregulating Crustacea, are characterized by complex, highly amplified basal and apical membrane surfaces, each intimately associated with an elevated number of mitochondria (Copeland, 1968; Copeland and Fitzjarrell, 1968; Gilles and Péqueux, 1986; Péqueux, 1995; McNamara and Lima, 1997; McNamara and Torres, 1999; Luquet et al., 1997; Luquet et al., 2002; Genovese et al., 2004).

Numerous studies have demonstrated that the basally located gill Na^+/K^+-ATPase drives active Na^+ uptake from dilute media into the hemolymph of hyperosmoregulating crustaceans (Péqueux, 1995; Zare and Greenaway, 1998; Lucu and Towle, 2003), and the same Na^+/K^+-ATPase powers active Na^+ extrusion into saline media in hyporegulating crustaceans (Martinez et al., 1998). In species such as the freshwater crayfish, an apically located V-ATPase appears to complement the Na^+/K^+-ATPase in energizing osmoregulatory ion uptake from highly dilute media (Zare and Greenaway, 1998; Weihrauch et al., 2001). Apical Na^+/H^+ exchangers and Na^+ channels also play a role in Na^+ uptake across the gill epithelia of many freshwater tolerant species (Weihrauch et al., 2001; Towle et al., 2001; Onken et al., 2003; Kirschner, 2004), whereas a $Na^+/K^+/2Cl^-$ symporter located in the basal membranes drives Cl^- and Na^+ extrusion across salt-secreting epithelia (Riestenpatt et al., 1996; Luquet et al., 2005). However, although the pathways and effectors of ion movements across crustacean gill epithelia are fairly well comprehended, the levels at which the molecular and kinetic alterations (Furriel et al., 2000; Mendonça et al., 2007; Santos et al., 2007; Belli et al., 2009) underlying osmoregulatory acclimation are modulated remain to be elucidated, particularly with regard to transcriptional and post-translational phenomena.

Recent studies have attempted to elucidate the molecular basis of ion transport in a few crustaceans by identifying, characterizing and quantifying the mRNA expression of candidate genes encoding

transporters, particularly in the gills of brachyuran crabs acclimated to concentrated or dilute media (Riestenpatt et al., 1996; Towle et al., 1997; Towle et al., 2001; Weihrauch et al., 2001; Luquet et al., 2005). Examples include: the Na^+/H^+ exchanger that participates in Na^+ uptake and acid–base and cell volume regulation (Towle et al., 1997); the Na^+/K^+-ATPase whose overall transport activity and α-subunit mRNA expression are altered during salinity acclimation (Lovett et al., 2006); the V-ATPase B subunit whose mRNA increases substantially in abundance during ion uptake from hyposmotic media (Weihrauch et al., 2001; Luquet et al., 2005); and the $Na^+/K^+/2Cl^-$ co-transporter involved in both salt uptake and excretion in hyper/hypo-osmoregulating crustaceans (Riestenpatt et al., 1996; Luquet et al., 2005).

The palaemonid shrimp constitute one of the most diverse and widespread taxons to have successfully invaded freshwater from the ancestral marine habitat (Sollaud, 1923; Jalihal et al., 1993; Murphy and Austin, 2005; Augusto et al., 2009), and extant species exhibit varying degrees of adaptation to low salinity environments, manifest in their diverse osmoregulatory abilities (Moreira et al., 1983; Freire et al., 2003; Freire et al., 2008b). Many freshwater species occur in neotropical latitudes and numerous species are present throughout the South American hydrographic basins, particularly in Brazilian river systems (Holthuis, 1952; Moreira et al., 1983; Bond-Buckup and Buckup, 1989; Pereira and Garcia, 1995). The neotropical palaemonids include species of *Palaemon*, *Palaemonetes* and *Macrobrachium* found from marine to freshwater environments, including coastal waters and estuaries, habitats that are characterized by elevated salinity fluctuation, and constitute a group that presents particularly attractive and convenient species in which to characterize adaptive osmoregulatory strategies (Freire et al., 2003; Freire et al., 2008b; Augusto et al., 2007; Augusto et al., 2009). The invasion of the freshwater environment by the palaemonid shrimp and the selection of species that maintain elevated extracellular ionic gradients appear to derive from adaptative advantages conferred by efficient mechanisms of anisosmotic extracellular regulation effected by transporter proteins, such as Na^+/K^+- and V-ATPase, that drive salt uptake in hyposmotic media and allow limited salt secretion in hyperosmotic media across ion transporting epithelia like the gills and the antennal glands (Freire et al., 2008a). The seven gill pairs present in palaemonid shrimp are not structurally or functionally differentiated into anterior 'respiratory' and posterior 'ion transporting' types as are often found in brachyuran crabs (Péqueux, 1995). Rather, all of the homogeneous gill lamellae perform the dual role of gas exchange and ion transport (Freire and McNamara, 1995; Mcnamara and Lima, 1997; Freire et al., 2008a) by means of a peculiar structural architecture. In *Macrobrachium* species, the gill epithelium consists of highly differentiated pillar cells that are structurally and functionally linked to an intralamellar septum (Belli et al., 2009), the invaginations of which house the Na^+/K^+-ATPase that drives salt uptake (McNamara and Torres, 1999). The surface area and thickness of the pillar cell flanges in *Macrobrachium olfersi*, which are augmented by extensive apical evaginations when in freshwater, decrease markedly on salinity acclimation (McNamara and Lima, 1997), accompanying the downregulation of ion uptake processes (Lima et al., 1997).

Many populations of the cinnamon shrimp *Macrobrachium amazonicum* are found in slowly flowing rivers near the sea and depend on brackish or estuarine water for complete larval development (McNamara et al., 1983; Moreira and McNamara, 1986). Others, however, are hololimnetic and spend their entire life cycle in freshwater several thousand kilometers from the sea, and in this case are completely independent of salt water for reproduction (Zanders and Rodriguez, 1992; Collart and Rabelo, 1996). Overall, the species is a good hyperosmotic and ionic regulator (Provérbio et al., 1990; Zanders and Rodriguez, 1992; Augusto et al., 2007) and exhibits some capability for isosmotic intracellular regulation that is dependent on muscle free amino acids (Augusto et al., 2007).

The present study examines the time course of osmoregulatory acclimation to elevated salinity in the diadromous, freshwater shrimp *M. amazonicum*. We evaluate alterations in hemolymph osmolality and in $[Cl^-]$, and in the mRNA expression and activity patterns of two fundamental ion transport proteins in the gill epithelium: Na^+/K^+-ATPase and V-ATPase. We also provide an ultrastructural analysis of the organization of the transport-related epithelial cell membrane systems, characterize V-ATPase kinetics and compare deduced amino acid sequences for the gill Na^+/K^+- and V-ATPases. These findings are brought together in an endeavor to elucidate the biochemical, transcriptional and ultrastructural underpinnings of salinity acclimation in freshwater palaemonid shrimp.

MATERIALS AND METHODS

Adult, intermolt, freshwater shrimp (*Macrobrachium amazonicum* Heller 1862), 10 to 15 cm in length, were collected using a builder's sieve from the marginal vegetation lining the outflow [salinity (S) <0.5‰, ~23°C] of the Santa Elisa reservoir (21°06′35.41″ S, 48°03′05.98″ W), a small man-made lake near Ribeirão Preto in northeastern São Paulo State, Brazil. In the laboratory, shrimp were held at ~25°C for up to 10 days under a natural light:dark photoperiod (14 h:10 h light:dark) in large, plastic 60-l tanks containing aerated water (<0.5‰ S) from a local spring, here termed 'freshwater', with hollow bricks as refuge. Shrimp were allotted at least two liters of water each, with a maximum of 15 shrimp held in each tank. The nocturnally active shrimp were fed in the evening with minced beef on alternate days, and uneaten fragments were removed the following morning.

Salinity acclimation, and osmotic and ionic regulation

To evaluate hemolymph osmotic and chloride regulatory capability, groups of 3–32 (mean ≈ 10) shrimp each were directly acclimated for 10 days from freshwater to media of 15 (450 mOsm kg^{-1} H_2O), 21 (630 mOsm kg^{-1} H_2O) or 25‰ S (750 mOsm kg^{-1} H_2O), prepared by diluting natural seawater (Maresias Beach seawater, 33.5‰ S) with freshwater and measured using an optical refractometer (±0.5‰ S precision; American Optical, Model 10419, Buffalo, NY, USA). Control shrimp were held in freshwater (<0.5‰ S, 15 mOsm kg^{-1} H_2O).

To accompany the events underlying the time course of direct salinity acclimation, hemolymph osmolality, $[Cl^-]$, and gill Na^+/K^+-ATPase activity and Na^+/K^+-ATPase α-subunit and V-ATPase B-subunit mRNA expression were quantified. Control shrimp were held in freshwater (time=0 h) and the experimental groups were sampled at 1 and 5 h and 1, 5 and 10 days after exposure to 25‰ S, a salinity that represents a rigorous osmotic challenge [12% mortality within 10 days; survival at 30‰ S is less than 10% by 10 days (Augusto et al., 2007)]. Gill V-ATPase activity was assayed in shrimp directly acclimated for 10 days from freshwater to 21‰ S; control shrimp were held in reservoir water.

Hemolymph samples were drawn by cardiac puncture with a #25-8 needle and an insulin syringe from each shrimp and frozen at –20°C prior to analysis. Hemolymph osmolality was measured in 10 μl aliquots using a vapor pressure micro-osmometer (Wescor Model 5500, Wescor Inc., Logan, UT, USA). Hemolymph $[Cl^-]$

was quantified by microtitration in 10 µl aliquots employing a modification (Santos and McNamara, 1996) of Schales and Schales (Schales and Schales, 1941) method, using *S*-diphenyl carbazone as the indicator and mercuric nitrate as the titrant.

Data for hemolymph osmolality and [Cl^-] after a 10-day acclimation period in the different salinities were fitted to second-order polynomial equations: $Y=a_2X^2+a_1X+a_0$, where a_2 is the quadratic coefficient, a_1 is the linear coefficient and a_0 is the constant (free) term. Isosmotic and iso-chloride points, i.e. the intercepts of the adjusted curves and the isosmotic and iso-chloride lines, were calculated according to Augusto et al. (Augusto et al., 2007). Osmotic and chloride regulatory capabilities are expressed numerically as the ratio of change in hemolymph osmotic or Cl^- concentration (Δ hemolymph mOsm kg^{-1} H_2O or mmol l^{-1} Cl^-) as a function of the change in osmotic or Cl^- concentration of the external medium (Δ medium mOsm kg^{-1} H_2O or mmol l^{-1} Cl^-), up to the isosmotic or iso-chloride point. A ratio of 1 indicates no regulation whereas values close to 0 indicate excellent regulatory capability (Freire et al., 2003).

Gill Na^+/K^+-ATPase activity

After chilling briefly on ice, the last four gill pairs from each of at least five shrimp acclimated for 1 and 5 h, or 1, 5 and 10 days, to 25‰ S were homogenized using a Potter homogenizer in homogenization buffer (20 mmol l^{-1} imidazole , 250 mmol l^{-1} sucrose and 6 mmol l^{-1} EDTA, pH 6.8; 20 ml buffer g^{-1} fresh tissue) containing a protease inhibitor cocktail (1 mmol l^{-1} benzamidine, 5 µmol l^{-1} antipain, 5 µmol l^{-1} leupeptin and 1 µmol l^{-1} pepstatin A; Calbiochem, San Diego, CA, USA). Aliquots were assayed spectrophotometrically at 25°C for total and ouabain-insensitive (2 mmol l^{-1} ouabain) ATPase activities using a pyruvate kinase/lactate dehydrogenase-linked assay in which ATP hydrolysis was coupled to NADH oxidation (Furriel et al., 2000; Masui et al., 2002). NADH oxidation was monitored at 340 nm ($\varepsilon_{340\,nm,pH\,7.5}$= 6200 $mmol^{-1}1cm^{-1}$) in a FEMTO 700 Plus spectrophotometer equipped with thermostatted cell holders. Standard conditions were 50 mmol l^{-1} Hepes/Tris, pH 7.5, 2 mmol l^{-1} ATP, 3 mmol l^{-1} $MgCl_2$, 10 mmol l^{-1} KCl, 40 mmol l^{-1} NaCl, 0.14 mmol l^{-1} NADH, 2 mmol l^{-1} PEP, 49 U PK and 94 U LDH in a final volume of 1.0 ml. The difference in activities measured with or without ouabain represents the Na^+/K^+-ATPase activity. One enzyme unit (U) is defined as the amount of enzyme that hydrolyzes 1.0 nmol of ATP per minute, at 25°C.

Total protein titers in the homogenates were measured according to Read and Northcote (Read and Northcote, 1981), using bovine serum albumin as the standard.

Gill V-ATPase activity

V-ATPase activities were measured in gill microsomes prepared from shrimp held in freshwater or directly acclimated to 21‰ S for 10 days. After brief chilling in crushed ice, all gill pairs were rapidly dissected on ice in homogenization buffer (20 mmol l^{-1} imidazole, pH 6.8, 250 mmol l^{-1} sucrose, 6 mmol l^{-1} EDTA). For each homogenate, the gills from 15 to 20 shrimp were diced and homogenized in homogenization buffer containing the protease inhibitor cocktail (see above, 20 ml buffer g^{-1} wet tissue), using a Potter homogenizer. After centrifuging the crude extract at 10,000 ***g*** for 35 min at 4°C, the supernatant was placed on crushed ice; the pellet was re-homogenized and re-centrifuged as above. The two supernatants were then pooled and centrifuged at 100,000 ***g*** for 2 h at 4°C. The resulting pellet was homogenized in 20 mmol l^{-1} imidazole buffer, pH 6.8, containing 250 mmol l^{-1} sucrose (15 ml buffer g^{-1} wet tissue). Finally, 0.5-ml aliquots were rapidly frozen in liquid nitrogen and stored at –20°C. No appreciable loss of microsomal activity was seen after storage for 2 months, either in shrimp maintained in freshwater or in those acclimated to 21‰ S. When required, the aliquots were thawed, placed on crushed ice and used immediately.

V-ATPase activity was assayed at 25°C using a PK/LDH linked system in which ATP hydrolysis was coupled to NADH oxidation (Furriel et al., 2000) monitored at 340 nm ($\varepsilon_{340\,nm,pH7.5}$= 6200 $mmol^{-1}1cm^{-1}$) in a FEMTO 700 Plus orthovanadate spectrophotometer equipped with thermostatted cell holders. Ortovanadate-insensitive ATPase activity corresponded to the ATPase activity estimated using 10 µmol l^{-1} sodium orthovanadate, which is sufficient to inhibit all P-type ATPases in the microsomal fractions from shrimp held at both salinities (Santos et al., 2007; Belli et al., 2009). Standard conditions were 50 mmol l^{-1} Hepes buffer, pH 7.5, 3 mmol l^{-1} ATP, 1.5 mmol l^{-1} $MgCl_2$, 0.2 mmol l^{-1} NADH, 3.2 mmol l^{-1} PEP, 49 U PK, 94 U LDH and 3 mmol l^{-1} KCl (to ensure adequate PK activity) in a final volume of 1.0 ml. Bafilomycin-insensitive ATPase activity was estimated as above employing 0.1 µmol l^{-1} bafilomycin A_1. The difference in activity measured with or without bafilomycin A_1 represents the V-ATPase activity. Controls without added enzyme were included in each experiment to quantify non-enzymatic substrate hydrolysis. One enzyme unit (U) is defined as the amount of enzyme that hydrolyzes 1.0 nmol of ATP per minute, at 25°C. Assays were performed on duplicate aliquots; each experiment was repeated using three different gill homogenates.

Amplification of partial Na^+/K^+-ATPase α-subunit and V-ATPase B-subunit cDNA sequences

Total RNA from the last four gill pairs of three shrimp held in freshwater (time=0 h, control) or acclimated for 1 and 5 h, or 1, 5 and 10 days, to 25‰ S was extracted under RNAse-free conditions in Trizol (Invitrogen Corporation, Carlsbad, CA, USA). After DNAse I RNAse-free treatment (Invitrogen) of 1 µg total RNA, mRNA reverse transcription was performed using oligo(dT) primers and Superscript II reverse transcriptase (Invitrogen), according to the manufacturer's instructions. Degenerate primers (see Table 1) employed successfully with crab species for the Na^+/K^+-ATPase α-subunit [primer pair NAK 10F/NAK 16R (Towle et al., 2001; Weihrauch et al., 2004)] and for the V-ATPase B-subunit [primer pair HAT F2/HAT R4 (Weihrauch et al., 2001; Weihrauch et al., 2004)] were used in a polymerase chain reaction (PCR) procedure using Taq polymerase 'High Fidelity' (Invitrogen) to amplify the partial cDNA sequences for both gill ion pumps. PCR products were analyzed by electrophoresis in 1% agarose gels using 1×Tris-borate-EDTA or 1×Tris-acetic acid-EDTA buffer (Ausubel et al., 1992). Nucleic acid bands in the gels were visualized by ethidium bromide staining (1 mg l^{-1}) and were photographed by employing a photodocumentation system.

Cloning and sequencing of PCR fragments

Individual PCR bands were cut from the agarose gels and the DNA was purified (Qiagen, Valencia, CA, USA). The purified PCR products were cloned into plasmid vectors (pCR 2.1 TOPO TA, Invitrogen) that were then used to transform electro-competent DH 10B *Escherichia coli*. The recombinant plasmids were extracted, analyzed by *Eco*RI restriction digestion and evaluated by agarose gel electrophoresis for the presence of an appropriately sized insert. Successful clones were sequenced (Genetic Analyzer, ABI PRISM Model 3100, Applied Biosystems, Foster City, CA, USA) using the dideoxynucleotide method (Sanger et al., 1977) employing the M13

forward and M13 reverse primers provided with the pCR 2.1 TOPO TA kit in the sequencing reaction. Fragment sequences were analyzed for open reading frames (ORF), and searches of GenBank using the BLAST algorithm (Altschul et al., 1990) revealed high similarity with sequences previously published for the Na^+/K^+-ATPase α-subunit and the V-ATPase B-subunit (Weihrauch et al., 2004). The sequences obtained (GenBank accession numbers: GQ329698, Na^+/K^+-ATPase α-subunit; GQ329699, V-ATPase B-subunit; GU366065, ribosomal protein L10) were then employed to design specific primers for *M. amazonicum* (see Table 1) using Oligo 4.0 software.

Quantitative RT-PCR (real-time PCR)

The relative abundance of Na^+/K^+-ATPase α-subunit mRNA and V-ATPase B-subunit mRNA in total RNA extracts was estimated by quantitative reverse transcription (RT) real-time PCR (Real Time 7500 PCR System, Applied Biosystems). Pools of the last four gill pairs from three to five shrimp were used for each time interval (time=0 h, control, freshwater; or acclimated for 1 and 5 h, or 1, 5 and 10 days, to 25‰ S); each measurement was repeated in triplicate. Real-time PCR reactions were performed using the Power SYBR Green PCR Master Mix Kit (Applied Biosystems) according to the manufacturer's instructions. The thermocycling procedure consisted of an initial step at 95°C for 10 min, followed by 40 cycles at 95°C for 15 s each and a final step at 60°C for 1 min. The RPL10 gene that encodes for ribosomal protein L10 was used as an internal control, and Na^+/K^+-ATPase α-subunit mRNA and V-ATPase B-subunit mRNA expression were normalized against the respective ribosomal protein L10 mRNA values. The coefficient of variation for RPL10 mRNA expression during the time course (0 to 240 h) of salinity acclimation was ≈6%. Specific primers for *M. amazonicum* L10 were designed from sequences originally amplified using *Callinectes sapidus* L10 specific primers (see Table 1) based on the complete nucleotide sequence for *C. sapidus* ribosomal protein L10 mRNA available from GenBank (AY822650.1).

Gill ultrastructure

The sixth gill, the largest and a typically osmoregulatory gill in palaemonid shrimp (Freire and McNamara, 1995; McNamara and Lima 1997; McNamara and Torres, 1999), was chosen to characterize the osmoregulatory epithelia. After removing the branchiostegites from shrimp held in freshwater, medial portions comprising about 10 lamellae each, taken from the sixth gill pair were dissected under primary fixative on ice (200 mmol l^{-1} paraformaldehyde, 250 mmol l^{-1} glutaraldehyde, 65 mmol l^{-1} NaCl, 5 mmol l^{-1} KCl, 1 mmol l^{-1} $MgCl_2$, 5 mmol l^{-1} $CaCl_2$ in 100 mmol l^{-1} sodium cacodylate, pH 7.4, estimated effective osmolality <450 mOsm kg^{-1} H_2O) and then fixed for 1.5 h on ice. The lamellae were then rinsed (3×5 min) in buffer solution alone and postfixed for 1.5 h in 1% osmium tetroxide in the same buffer system on ice. Subsequent dehydration, embedding and sectioning procedures followed those of McNamara and Torres (McNamara and Torres, 1999). After staining with aqueous uranyl acetate and Reynolds' lead citrate (Reynolds, 1963), 80-nm thin sections were examined at an accelerating voltage of 100 kV using a Philips EM 208 electron microscope.

Statistical analyses

Data are given in the text as the mean ± s.e.m. (*N*). After satisfying criteria for normality of distribution and equality of variance, data sets were analyzed using a one-way analysis of variance (salinity or time) followed by the Student–Newman–Keuls multiple comparisons procedure to locate significantly different means (SigmaStat 2.03 software package); a minimum significance level of P=0.05 was employed.

RESULTS

Hemolymph osmotic and ionic regulatory capability

In freshwater (<0.5‰ S), *Macrobrachium amazonicum* maintains a hemolymph osmolality of 400±9 mOsm kg^{-1} H_2O (*N*=12). After a 5- to 10-day acclimation to 15, 21 or 25‰ S, osmolality increased significantly to 509±16 (*N*=3), 660±5 (*N*=32) and 742±3 mOsm kg^{-1} H_2O (*N*=8), respectively, and was hyper-regulated up to the isosmotic point at 720 mOsm kg^{-1} H_2O (24.0‰ S; Fig. 1). Osmoregulatory capability (Δ hemolymph osmolality/Δ medium osmolality=0.45) was modest.

Hemolymph chloride concentration in freshwater was 218±18 mmol l^{-1} Cl^- (*N*=17) and 247±23 mmol l^{-1} (*N*=3) in 15‰ S, increasing to 296±9 (*N*=11) and 341±12 mmol l^{-1} Cl^- (*N*=8) after 10-days acclimation to 21 and 25‰ S, respectively. Chloride concentration was hyper-regulated up to the iso-chloride point at 249.6 mmol l^{-1} Cl^- (15.6‰ S) and was hyporegulated in 20 and 25‰ S (Fig. 1). Chloride regulatory capability was strong (0.13).

When *M. amazonicum* was transferred directly from freshwater to 25‰ S (750 mOsm kg^{-1} H_2O, 400 mmol l^{-1} Cl^-; Fig. 2A), hemolymph osmolality increased to 450±9 mOsm kg^{-1} H_2O (*N*=9) within 1 h. This level was sustained at 5 h (435±15 mOsm kg^{-1} H_2O, *N*=9), increased markedly to 722±21 mOsm kg^{-1} H_2O (*N*=12) by 1 day, sustained at 5 days (745±5 mOsm kg^{-1} H_2O, *N*=13), and remained unchanged at 10 days.

During the time course of direct acclimation to 25‰ S (Fig. 2B), hemolymph chloride concentration initially decreased significantly within 1 h to 183±5 mmol l^{-1} Cl^- (*N*=7), returned to the freshwater value (229±17 mmol l^{-1} Cl^-, *N*=7) by 5 h, then increased markedly

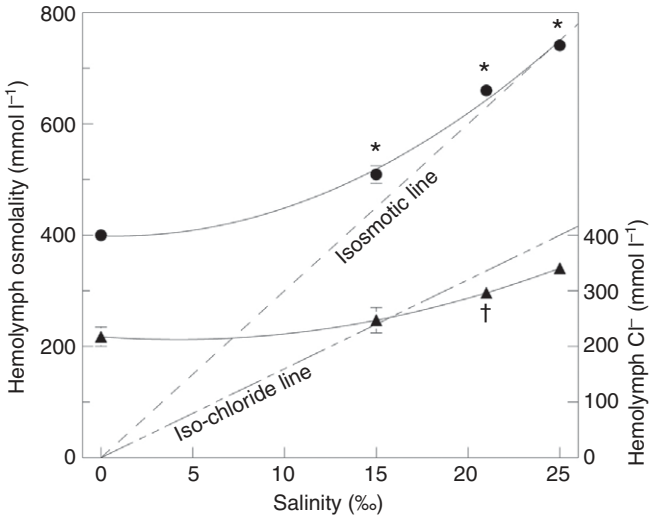

Fig. 1. Hemolymph osmotic and chloride regulatory capability in the freshwater shrimp *Macrobrachium amazonicum* after direct acclimation for 10 days to 21 or 25‰ salinity (S). Data are mean ± s.e.m. (*N*=3–32) and have been fitted with second order polynomial equations (osmolality, $y=0.60x^2 - 1.01x + 398.69$, R^2= 0.993, closed circles; chloride, $y=0.30x^2 - 2.46x + 217.7$, R^2=0.999, closed triangles). Calculated isosmotic (1‰ S=30 mOsm kg^{-1} H_2O) and iso-chloride (1‰ S=16 mmol l^{-1} Cl^-) points are 720 mOsm kg^{-1} H_2O and 265 mmol l^{-1} Cl^-, respectively. *P≤0.05 compared with preceding value; †P≤0.05 compared with 0‰ S (one-way ANOVA, SNK). Where lacking, error bars are smaller than symbols used.

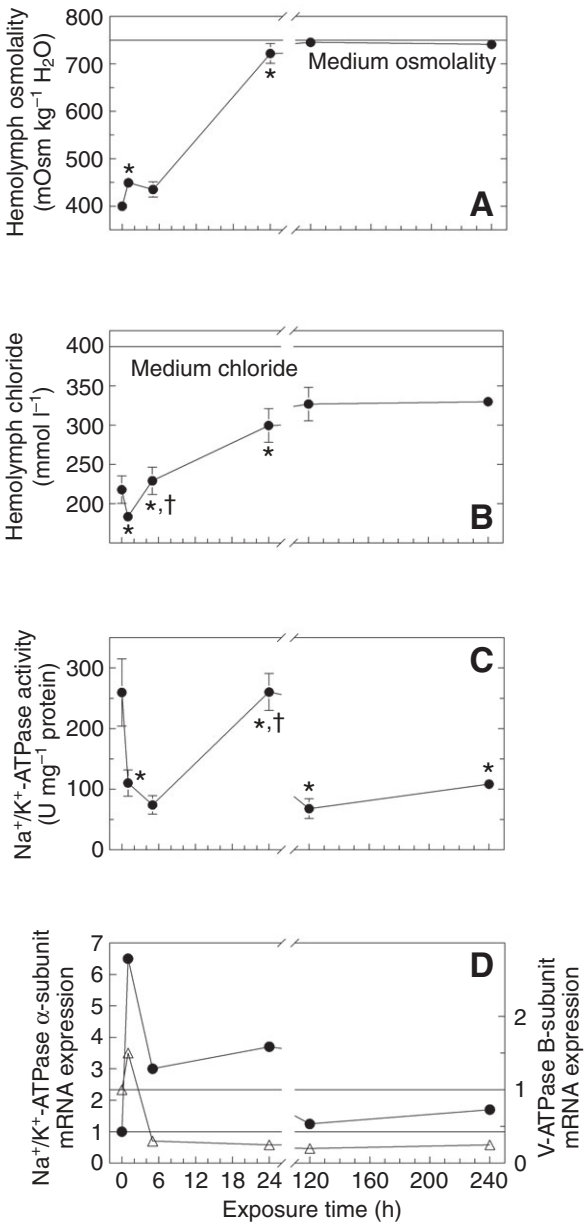

Fig. 2. Immediate (0, 1, 5 and 24 h) and long-term (5 and 10 day) time course of direct acclimation for 10 days to 25‰ salinity (750 mOsm kg^{-1} H_2O, 400 mmol l^{-1} Cl^-) in the freshwater shrimp *Macrobrachium amazonicum*. (A) Alterations in hemolymph osmolality (mean ± s.e.m., *N*=7–10). (B) Alterations in hemolymph chloride (mean ± s.e.m., *N*=7–10). (C) Alterations in Na$^+$/K$^+$-ATPase specific activity in gill homogenates (mean ± s.e.m., *N*=4–5). (D) Relative expression of Na$^+$/K$^+$-ATPase α-subunit (closed circles) and V-ATPase B-subunit (open triangles) mRNA in gill homogenates (normalized to ribosomal protein L10 mRNA). Data are the means of triplicate measurements performed on single samples pooled from three to five shrimp. *P≤0.05 compared with immediately preceding value; †P>0.05 compared with control value (time=0; one-way ANOVA, SNK).

to 300±21 mmol l^{-1} Cl^- (*N*=7) after 1 day; the concentration was sustained at 327±21 mmol l^{-1} Cl^- (*N*=10) at 5 days, and remained unchanged at 10 days.

Gill Na$^+$/K$^+$-ATPase specific activity

After direct transfer from freshwater to 25‰ S (350 mmol l^{-1} Na^+; Fig. 2C), Na$^+$/K$^+$-ATPase specific activity in *M. amazonicum* gill homogenates initially decreased rapidly from 260±56 U mg^{-1} protein (*N*=5) in freshwater to 110±22 U mg^{-1} protein (*N*=5; P<0.05) by 1 h, and to 74±15 U mg^{-1} protein (*N*=5) by 5 h. Na$^+$/K$^+$-ATPase activity then returned to freshwater levels 1 day after transfer (260±31 U mg^{-1} protein, *N*=5), decreasing again significantly by 5 days (68±16 U mg^{-1} protein, *N*=5), and showing a slight but significant increase at 10 days (108±9 U mg^{-1} protein, *N*=4).

Sequencing and expression of gill Na$^+$/K$^+$-ATPase α-subunit and V-ATPase B-subunit mRNA

PCR amplification employing the degenerate primer pair combinations NAK 10F/NAK 16R and HATF2/HATR4 resulted in single amplification products for each target transporter transcript, which were gel purified, cloned and sequenced. The RPL10_Cs_F/RPL10_Cs_R primer combination produced a single product for the target internal control transcript and also was purified, cloned and sequenced (deposited under GenBank accession numbers: Na$^+$/K$^+$-ATPase α-subunit, GQ329698; V-ATPase B-subunit, GQ329699; ribosomal protein L10, GU366065). The respective nucleotide sequences were translated to ORFs that yielded high-scoring BLASTX matches to known sequences in GenBank (http://www.ncbi.nlm.nih.gov/), corresponding to each transporter and ribosomal protein L10 transcript. The specific primers for each gene were designed based on the sequences amplified for *M. amazonicum* (Table 1).

Alignment of deduced amino acid sequences for the ion transporters from *M. amazonicum* with those of other organisms revealed conserved regions possibly involved in ATP binding and hydrolysis (Figs 3, 4). Close identities for the partial *M. amazonicum* Na$^+$/K$^+$-ATPase α-subunit sequence were found with those for the estuarine crab *Neohelice* (previously *Chasmagnathus*) *granulata* (93.7%, AF548369.1), the diadromous freshwater crab *Eriocheir sinensis* (93.3%, AF301158.1), the intertidal crab *Pachygrapsus marmoratus* (93.3%, DQ173925.2), the marine lobster *Homarus americanus* (93.3%, AY140650.1), the true freshwater crab *Dilocarcinus pagei* (92.1%, AF409119.1), the fruit fly *Drosophila melanogaster* (81.6%, AF044974.1), *Homo sapiens* (72.6%, X12910.1) and the African clawed frog *Xenopus laevis* (70%, BC043743.1). For the deduced amino acid sequence of the *M. amazonicum* V-ATPase B subunit, very close percentage identities (99.1%) were found with those of *D. pagei* (AF409118.1), the euryhaline intertidal crab *Carcinus maenas* (AF189779.2), the marine rock crab *Cancer irroratus* (AF189781.1) and the terrestrial isopod *Porcellio scaber* (AY278992.1). Close identities were also evident with *N. granulata* (98.3%, AF189783.1), *X. laevis* (94.0%, BC046738.1) and *H. sapiens* (94.9%, BC007309.1).

The deduced amino acid sequence for *M. amazonicum* ribosomal protein L10 (Fig. 5), our internal control gene, showed elevated identity with the estuarine blue crab *Callinectes sapidus* (94.8%, AY822650.1), the false skin beetle *Biphyllus lunatus* (89.7%, M049016.1), the tobacco budworm moth *Heliothis virescens* (86.9%, AF368032.1), the silk moth *Bombyx mori* (87.9%, AY769278.1), the western clawed frog *X. tropicalis* (82.8%, NM_001004965.1) and *H. sapiens* (82.8%, CH471172.2).

The relative expression of Na$^+$/K$^+$-ATPase α-subunit mRNA in the gills (normalized to ribosomal protein L10 mRNA) increased markedly by 6.5-fold after 1 h of direct exposure to 25‰ S (Fig. 2D). However, the relative expression of the α-subunit mRNA levels then decreased to 3.0- and 3.7-fold after 5 h and 1 day, respectively, continuing to decrease until days 5 and 10, when the relative expression was just 1.25- and 1.7-fold greater, respectively, than in shrimp in freshwater.

Table 1. Degenerate and specific oligonucleotide primers used to amplify Na^+/K^+-ATPase α-subunit, V-ATPase B-subunit and ribosomal protein L10 cDNA from *Macrobrachium amazonicum* gills

Primer	Nucleotide sequence (5′–3′)	Amplicon (bp)
Na^+/K^+-ATPase		
Degenerate sense primer NaK_10F	ATGACIGTIGCICAYATG	707
Degenerate antisense primer NaK_16R	GGRTGRTCICCIGTIACCAT	
Specific sense primer NaK_Mam_F	TACACGCTCACCAAGACCTCCC	102
Specific antisense primer NaK_Mam_R	TGGCTTGCGGTGATGTTAAGGG	
V-ATPase		
Degenerate sense primer HAT_F2	GCNATGGGNGTNAAYATGGA	392
Degenerate antisense primer HAT_R4	TGNGTDATRTCRTCGTTNGG	
Specific sense primer V_Mam_F	TTCCTTCTACTCGACCGGCACG	81
Specific antisense primer V_Mam_R	TGCCAGGTAGACGTGGTTTCCC	
Ribosomal protein L10 (control)*		
Sense primer RPL10_Cs_F	AAGAACTGCGGCAAGGACCAGTTCC	350
Antisense primer RPL10_Cs_R	CGGTCAAACTTGGTAAAGCCCCACTT	
Specific sense primer RPL10_Mam_F	AAATGTTGTCGTGTGCTGGTGC	91
Specific sense primer RPL10_Mam_R	ATTCTTACACGTGCAACCGTGC	

*The specific primers for *M. amazonicum* ribosomal protein L10 were designed from sequences originally amplified using *Callinectes sapidus* L10 specific primers (sense/antisense sequences RPL10_Cs_F and RPL10_Cs_R).
D replaces A/G/T; N and I replace A/C/G/T; R replaces A/G; Y replaces C/T.

Gill V-ATPase B-subunit mRNA expression increased 1.5-fold after 1 h of exposure to 25‰ S (Fig. 2D). B-subunit mRNA levels then decreased considerably to 0.3- and 0.25-fold after 5 h and 1 day, respectively, continuing to decrease by days 5 and 10, when expression of the V-ATPase B-subunit mRNA was just 0.2- to 0.25-fold that of shrimp in freshwater.

Kinetic characterization of gill V-ATPase specific activity

Stimulation of V-ATPase activity in gill microsomes from *M. amazonicum* maintained in freshwater by ATP (Fig. 6A) and Mg^{2+} (Fig. 6B), each under saturating concentrations of the other, followed simple saturation curves, both obeying cooperative kinetics (ATP n_H=2.8, Mg^{2+} n_H=3.5). Specific V-ATPase activities were

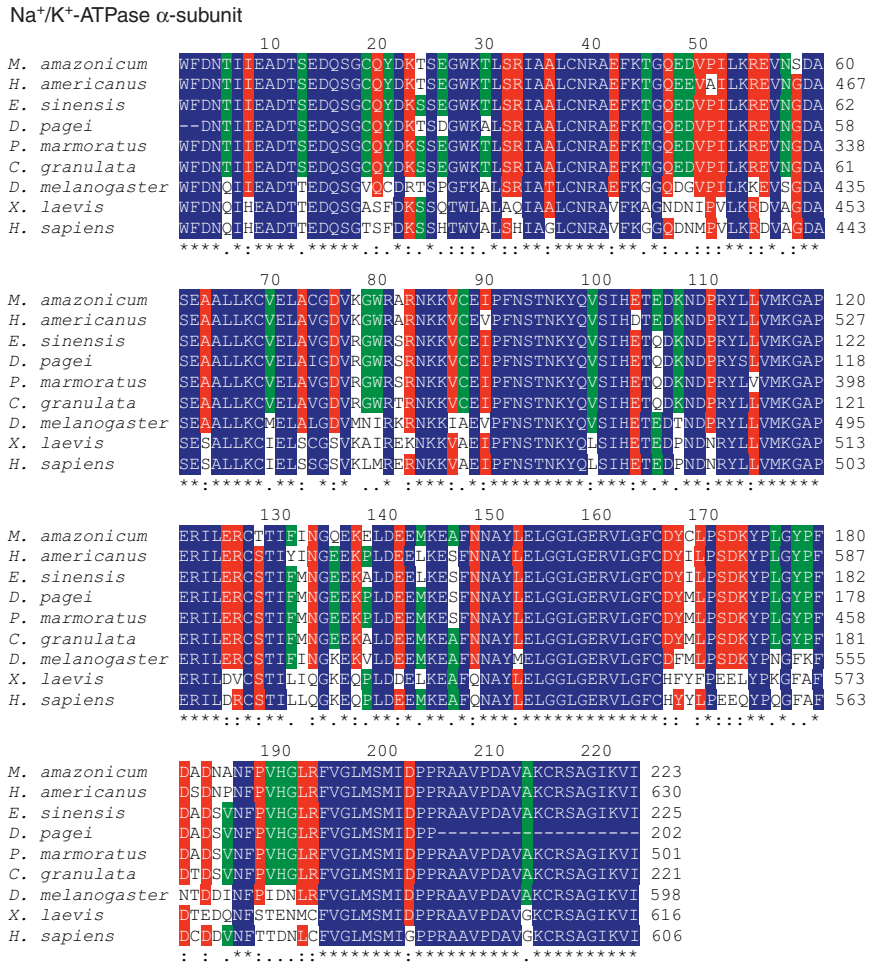

Fig. 3. Multiple alignment of the deduced amino acid sequence for the Na^+/K^+-ATPase α-subunit from the gill tissue of the freshwater shrimp *Macrobrachium amazonicum* compared with that of other arthropods [*Homarus americanus*, *Eriocheir sinensis*, *Dilocarcinus pagei*, *Pachygrapsus marmoratus, Neohelice (Chasmagnathus) granulata*, *Drosophila melanogaster*] and vertebrates (*Xenopus laevis*, *Homo sapiens*). The sequence corresponds to a section of cytosolic loop 2 between transmembrane helices 4 and 5, located just posterior to the site of ATP hydrolysis (Chung and Lin, 2006). Alignment was performed using the Clustal W software package (http://www.ebi.ac.uk/clustalw). Blue (*) indicates 100% identity; red (:) from 75 to 90% identity with one or two different amino acids; green (.) from 50 to 70% identity with three different amino acids; no color and no character indicate less than 50% identity with more than three different amino acids. A, alanine; C, cysteine; D, aspartate; E, glutamate; F, phenylalanine; G, glycine; H, histidine; I, isoleucine; K, lysine; L, leucine; M, methionine; N, asparagine; P, proline; Q, glutamine; R, arginine; S, serine; T, threonine; V, valine; W, tryptophan; Y, tyrosine. Numbers on the right indicate the position of the amino acid in the respective GenBank sequence.

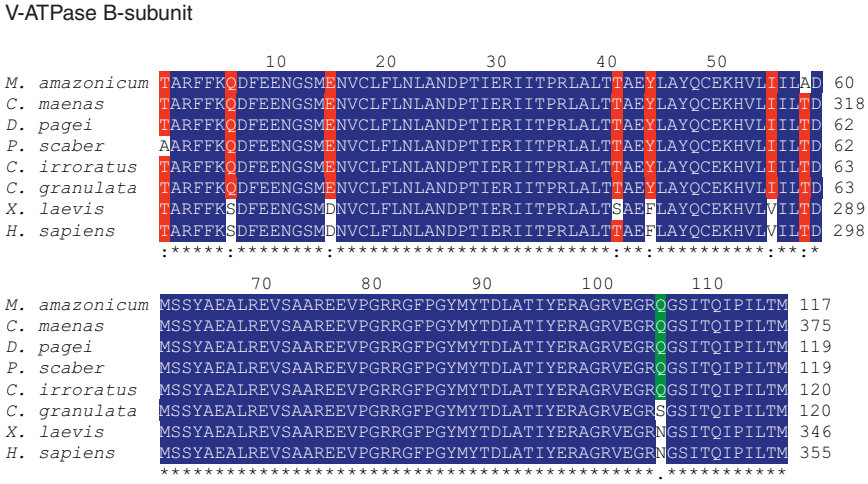

Fig. 4. Multiple alignment of the deduced amino acid sequence for the V-ATPase B-subunit from the gill tissue of the freshwater shrimp *Macrobrachium amazonicum* compared with that of other arthropods [*Carcinus maenas*, *Dilocarcinus pagei*, *Porcellio scaber*, *Cancer irroratus*, *Neohelice (Chasmagnathus) granulata*] and vertebrates (*Xenopus laevis*, *Homo sapiens*). Alignment was performed using the Clustal W software package (http://www.ebi.ac.uk/clustalw). Blue (*) indicates 100% identity; red (:) from 75 to 90% identity with one or two different amino acids; green (.) from 60 to 70% identity with three different amino acids. A, alanine; C, cysteine; D, aspartate; E, glutamate; F, phenylalanine; G, glycine; H, histidine; I, isoleucine; K, lysine; L, leucine; M, methionine; N, asparagine; P, proline; Q, glutamine; R, arginine; S, serine; T, threonine; V, valine; W, tryptophan; Y, tyrosine. Numbers on the right indicate the position of the amino acid in the respective GenBank sequence.

22.7±1.3 U mg^{-1} protein with an apparent affinity of 1.11±0.06 mmol l^{-1} for ATP, and 23.3±1.2 U mg^{-1} protein with $K_{0.5}$=0.44±0.02 mmol l^{-1} for Mg^{2+}.

Bafilomycin A_1 concentrations around 0.1 µmol l^{-1} inhibited approximately 40% of the orthovanadate-insensitive ATPase activity in microsomal fractions from shrimp held in freshwater (Fig. 6C), corresponding to a V-ATPase activity of 23.0±1.5 U mg^{-1} protein. The calculated apparent dissociation constant (K_I) for bafilomycin A_1 inhibition was 3.97±0.32 nmol l^{-1} (Fig. 6C, inset). By contrast, in microsomal fractions from shrimp acclimated to 21‰ S, bafilomycin A_1 concentrations up to 1 µmol l^{-1} had no effect on the orthovanadate-insensitive ATPase activity (Fig. 6C), demonstrating a drastic reduction in V-ATPase activity in response to salinity acclimation.

Gill epithelial ultrastructure

The symmetrical epithelium underlying the fine cuticle on either side of the gill lamella consists exclusively of extensive, apical pillar cell flanges. At semi-regular intervals, opposing pillar cell bodies protrude into the hemolymph space that is further divided by an intralamellar septum, forming a series of capillary-like lacunae through which the hemolymph flows (Fig. 7A).

The pillar cells are highly differentiated, each consisting of a stubby perikaryon (9.8±0.4 µm diameter, *N*=5) containing the spherical, basal nucleus, and thick, radially projecting, apical flanges (2.6±0.1 µm thickness, *N*=5). The cytoplasm above the perikaryon and within the flanges contains numerous mitochondria, abundant rough endoplasmic reticulum (RER) cisternae, polyribosomes and small vesicles with a visible cytoskeleton of microtubules and microfilaments (Fig. 7B). The apical membrane is greatly amplified by numerous evaginations (0.5±0.1 µm height, *N*=5; Fig. 7B,C), whereas the lower flange membrane lying against the basal lamina facing the hemolymph is not augmented at all (Fig. 7C). The flanges are attenuated at their periphery, adjacent plasmalemmae forming junctional complexes consisting of a desmosome-like macula, followed by a lengthy septate junction and a region of interdigitating, apposed membranes (Fig. 7B). The pillar cell bodies project into the hemolymph space and establish intimate contact with the intralamellar septal cells (Fig. 7A) by means of numerous, dense, interdigitating junctions (Fig. 7D) that form a narrow extracellular

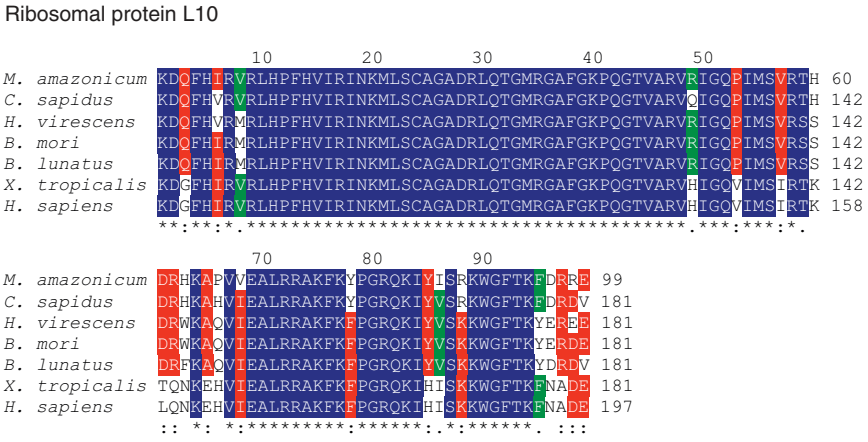

Fig. 5. Multiple alignment of the partial deduced amino acid sequence for the ribosomal protein L10 from the gill tissue of the freshwater shrimp *Macrobrachium amazonicum* compared with that of other arthropods (*Callinectes sapidus*, *Biphyllus lunatus*, *Heliothis virescens*, *Bombyx mori*) and vertebrates (*Xenopus tropicalis*, *Homo sapiens*). Alignment was performed using the Clustal W software package (http://www.ebi.ac.uk/clustalw). Blue (*) indicates 100% identity; red (:) from 70 to 85% identity with one or two different amino acids; green (.) <60 % identity with three different amino acid; no color and no character indicates less than 50% identity with more than three different amino acids. A, alanine; C, cysteine; D, aspartate; E, glutamate; F, phenylalanine; G, glycine; H, histidine; I, isoleucine; K, lysine; L, leucine; M, methionine; N, asparagine; P, proline; Q, glutamine; R, arginine; S, serine; T, threonine; V, valine; W, tryptophan; Y, tyrosine. Numbers on the right indicate the position of the amino acid in the respective GenBank sequence.

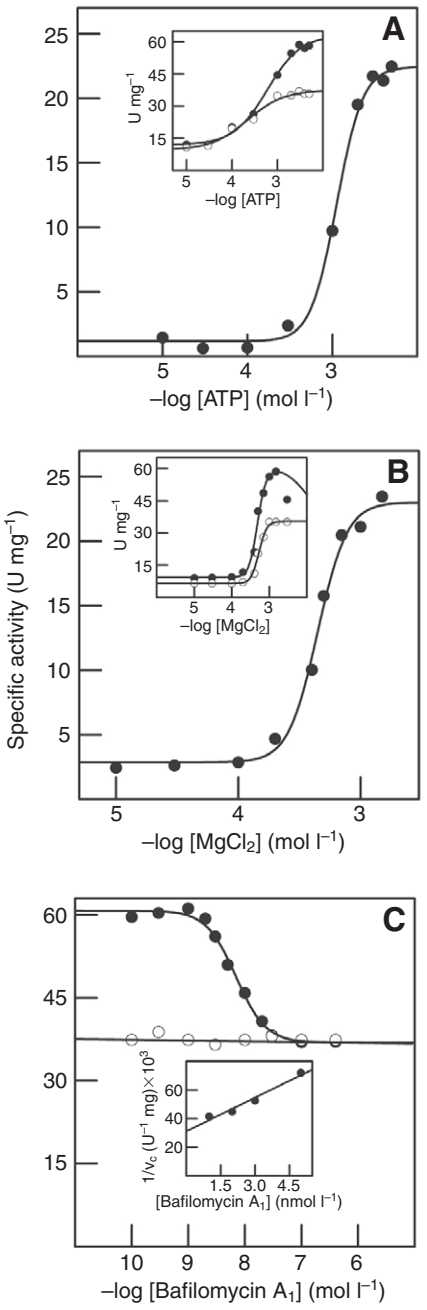

Fig. 6. Kinetic characterization of V-ATPase activity in microsomal gill fractions from *Macrobrachium amazonicum*. Modulation of V-ATPase activity by ATP (A) and magnesium ions (B) in shrimp held in freshwater, and (C) effect of bafilomycin A_1 on orthovanadate-insensitive ATPase activity in shrimp held in freshwater (closed circles) or acclimated to 21‰ salinity for 10 days (open circles). Activity was assayed continuously at 25°C in 50 mmol l^{-1} Hepes buffer, pH 7.5, in a final volume of 1.0 ml. Modulation of V-ATPase activity by ATP and Mg^{2+} was evaluated under optimal concentrations of the other, and the effect of bafilomycin A_1 on orthovanadate-insensitive ATPase activity was assayed under optimal concentrations of ATP and Mg^{2+}. Inset to A: effect of ATP concentration on bafilomycin-insensitive (open circles) and orthovanadate-insensitive (closed circles) ATPase activity. Inset to B: effect of Mg^{2+} concentration on bafilomycin-insensitive (open circles) and orthovanadate-insensitive (closed circles) ATPase activity. Inset to C: Dixon plot for estimation of K_I for bafilomycin A_1 in which v_c is the reaction rate corresponding to V-ATPase activity alone in microsomes from shrimp held in freshwater. Experiments were performed using duplicate aliquots from three different gill homogenates; representative curves for a single homogenate in each condition are given.

space. The septum is extensive and non-fenestrated, and the thick septal cells are characterized by abundant mitochondria, each surrounded by a deep invagination of the plasmalemma that considerably amplifies their surface area (Fig. 7D). The ultrastructural characteristics of these two cell types are typical of an ion-transporting epithelium.

DISCUSSION

Despite its ample geographical distribution and the wide salinity range encountered throughout its natural habitats, including continental waters and estuaries, the diadromous freshwater shrimp *Macrobrachium amazonicum* strongly hyper-regulates its hemolymph osmolality (≈400 mOsm kg^{-1} H_2O) against freshwater (see also Proverbio et al., 1990; Zanders and Rodriguez 1992; Augusto et al., 2007). Similarly elevated osmotic gradients are typical of neotropical *Macrobrachium* species, such as the coastal diadromous *M. heterochirus* (425 mOsm kg^{-1} H_2O), *M. acanthurus* (440 mOsm kg^{-1} H_2O) and *M. olfersi* (340 mOsm kg^{-1} H_2O), and the hololimnetic *M. potiuna* (493 mOsm kg^{-1} H_2O) and *M. brasiliensis* (412 mOsm kg^{-1} H_2O) (Moreira et al., 1983; Lima et al., 1997; Freire et al., 2003). In saline media, *M. amazonicum* hyper-regulates hemolymph osmolality up to isosmoticity at 736 mOsm kg^{-1} H_2O (24.5‰ S), iso- or slightly hypo-conforming thereafter. However, its osmoregulatory capability (0.45; Δ hemolymph mOsm kg^{-1} H_2O: Δ external medium mOsm kg^{-1} H_2O) is modest compared to that of other palaemonids, such as *M. olfersi* (0.33), *M. potiuna* (0.08), *M. brasiliensis* (0.24), *Palaemon pandaliformis* (0.20, estuarine) and *P. northropi* (0.20, marine intertidal) (Freire et al., 2003), that encounter comparable salinities over part of their ranges.

By contrast, hemolymph Cl^- in *M. amazonicum* is strongly hyper-regulated in freshwater (218 mmol l^{-1} Cl^-) and modestly hyporegulated at elevated salinity, the more efficient hemolymph Cl^- regulatory capability (0.18; Δ hemolymph mmol l^{-1} Cl^-: Δ external medium mmol l^{-1} Cl^-) suggesting independent regulatory mechanisms of the major hemolymph ions (Na^+ and Cl^-), as Na^+ constitutes most of the remaining hemolymph osmolality (Augusto et al., 2007). Furthermore, whereas hemolymph osmolality increases steadily to isosmoticity within 5 days at 25‰ S, hemolymph chloride initially decreases markedly, remaining well below external chloride after acclimation, indicating putative chloride secretory ability.

In freshwater, these strong osmotic and Cl^- gradients (see Fig. 1) are sustained by elevated Na^+/K^+- and V-ATPase activities. The initial rapid decrease in *M. amazonicum* gill Na^+/K^+-ATPase activity after 1 to 5 h of exposure to 25‰ S might result from a direct modulation of enzyme activity by substrate and ions, from increased hemolymph osmolality (Onken, 1996) and/or from hormonally regulated phosphorylation of this P-type ATPase. Na^+ and Cl^- uptake, dependent on increased gill Na^+/K^+-ATPase activity, is regulated by cell signaling *via* dopamine and norepinephrine linked to cyclic adenosine monophosphate transduction cascades in hyperegulating brachyuran crabs like *Carcinus maenas* (Zatta, 1987; Sommer and Mantel, 1991; Sommer and Mantel, 1988), *Callinectes sapidus* (Lohrmann and Kamemoto, 1987) and *Eriocheir sinensis* (Riestenpatt et al., 1994).

Despite the early decrease in Na^+/K^+-ATPase activity, there is a very rapid and substantial increase in gill Na^+/K^+-ATPase α-subunit mRNA expression after 1 h (6.5-fold), and 5 and 24 h (3- to 4-fold), which appears to sustain the subsequent increase in Na^+/K^+-ATPase activity after 24 h of exposure, suggesting the synthesis of new enzyme molecules (see Lovett et al., 2006). The lag between increased mRNA expression and measured Na^+/K^+-ATPase activity might reflect the interval between nuclear mRNA transcription, translational regulatory processes and protein

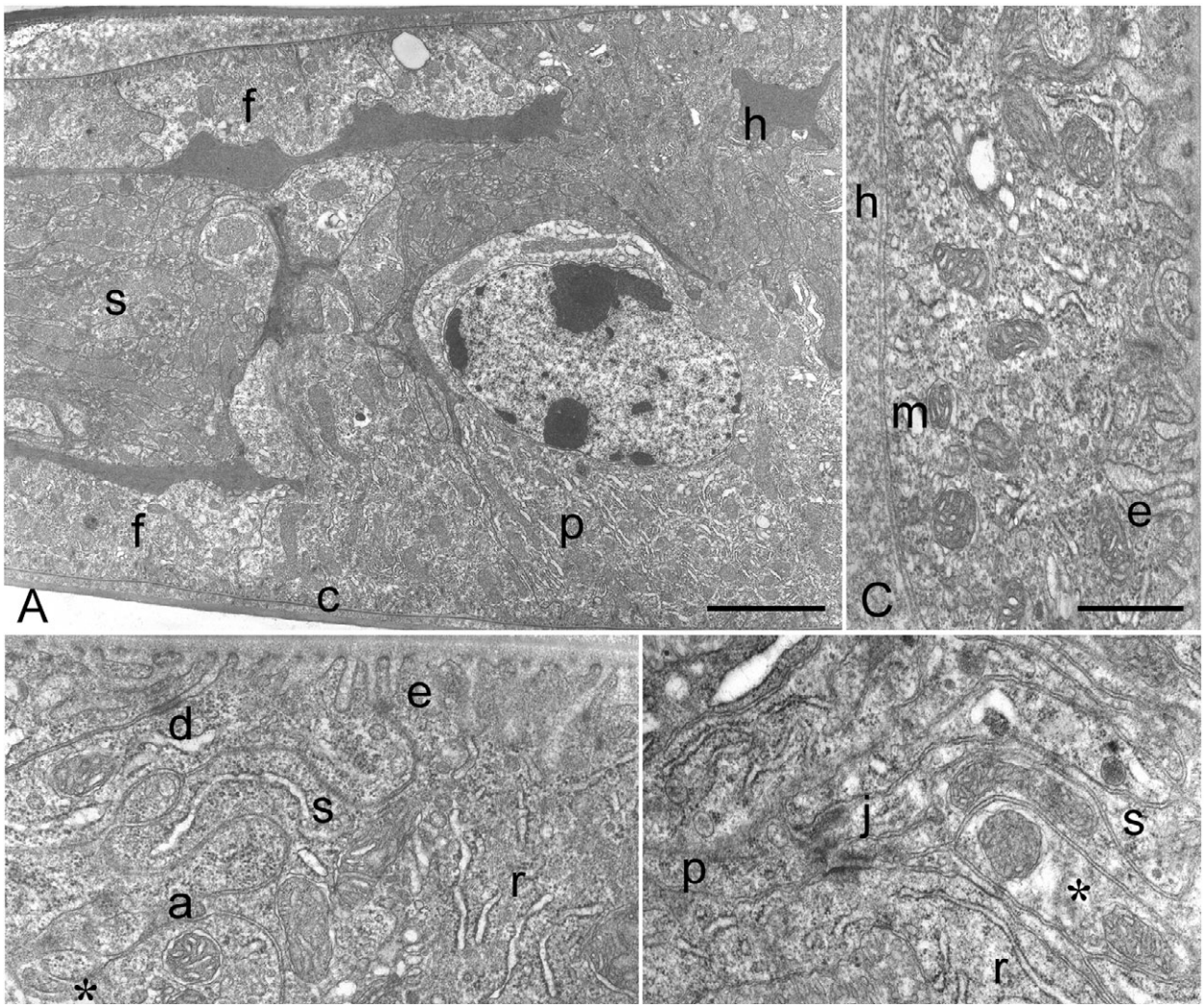

Fig. 7. Ultrastructure of the gill epithelium from *Macrobrachium amazonicum* in freshwater. (A) Transverse section of gill long axis showing overall lamellar architecture. The epithelium below the fine cuticle (c) consists of apical pillar cell flanges (f), and perikarya (p) that abut on the intralamellar septum (s), forming irregular hemolymph lacunae (h). (B) Junctional complex formed between membranes of adjacent pillar cell flanges showing an apical desmosome-like macula (d) at the base of the apical evaginations (e), a septate junction (s) and a stretch of closely apposed membranes (a) leading to the hemolymph space (*). Note the organelle rich cytoplasm containing mitochondria, vesicles and RER cisternae (r). (C) Apical flange showing well-developed evaginations (e) below the endocuticle, and the simple lower flange membrane (m) lying on the basal lamina facing the hemolymph (h). (D) Junctional interface (j) between a pillar cell base (p), characterized by electron dense cytoplasm and RER cisternae (r), and an electron lucent intralamellar septal cell (s) exhibiting mitochondria enclosed within membrane invaginations (*). Scale bars: in A, 3 μm; in B and D, 0.5 μm; in C, 1 μm.

activation in the Golgi cisternae and endoplasmic reticulum, and insertion of the enzyme into the septal cell membranes. There is a 7-day delay between increased gill mRNA levels and increased Na^+/K^+-ATPase activity in the euryhaline crab *Scylla paramamosain* acclimated to dilute media (Chung and Lin, 2006). Lucu and Flik (Lucu and Flik, 1999) suggest that increased gill Na^+/K^+-ATPase activity in *C. maenas* during rapid (4 h) responses results from pre-existing enzyme or recruitment of silenced enzyme, followed by new enzyme production within three weeks *via* mRNA transcription.

Even though it initially declines, gill Na^+/K^+-ATPase activity in *M. amazonicum* does appear to underlie hemolymph Cl^- hyporegulation, as the Na^+/K^+-ATPase also plays an important role in hyposmotic regulatory mechanisms (Kamemoto, 1991; Martinez et al., 1998; Luquet et al., 2002) and active salt secretion. The slow early increase in hemolymph [Cl^-] seen up to 24 h of exposure in *M. amazonicum* is accompanied by the strong recovery of Na^+/K^+-ATPase activity, which provides for stable [Cl^-] hyporegulation after 5 and 10 days of exposure. Although Na^+/K^+-ATPase activities are subsequently reduced over this time interval, these low levels seem sufficient to sustain the modest Cl^- gradient (Δ 60 mmol l^{-1} Cl^-) maintained in 25‰ S (cf. Δ 210 mmol l^{-1} Cl^- in freshwater, Fig. 2B,C). NaCl secretion, employing a basolateral $Na^+/K^+/2Cl^-$ symporter powered by Na^+ and K^+ turnover *via* the basal Na^+/K^+-ATPase and K^+ channels, has been described in fish gills (Evans et al., 1999), elasmobranch rectal gland (Riordan et al., 1994) and avian salt glands (Lowy et al., 1989). In the crustacean gill, electrophysiological data suggest a $Na^+/K^+/2Cl^-$ symporter in *Carcinus maenas* (Riestenpatt et al., 1996), and molecular cloning studies reveal expression of a $Na^+/K^+/2Cl^-$ symporter in *Neohelice (Chasmagnathus) granulata* and suggest that salt secretion is associated with increased Na^+/K^+-ATPase activity during exposure to hyperosmotic salinity (45‰ S) (Luquet et al., 2005). The Na^+/K^+-ATPase is thus essential for both hyper- and hypo-ionic regulation.

However, the enzyme itself does not define the ensuing directionality of net transport. This task falls to the $Na^+/K^+/2Cl^-$ symporter usually found at two different locations in vertebrate salt-transporting epithelial cells: an apical position drives NaCl uptake, whereas a basolateral setting powers NaCl secretion (Mount et al., 1998).

Isosmoticity in *M. amazonicum* (≈740 mOsm kg^{-1} H_2O after 5–10 days of exposure to 25‰ S) is accompanied by a marked reduction in gill Na^+/K^+-ATPase activity, whereas gill Na^+/K^+-ATPase α-subunit mRNA expression becomes reduced from the initially elevated post-exposure levels (up to 24 h) to values similar to those seen in freshwater, consistent with the upregulation of active salt secretion, particularly of Cl^- (Δ 60 mmol l^{-1} Cl^-) because hemolymph osmolality lies just 10 mOsm kg^{-1} H_2O below ambient osmolality (750 mOsm kg^{-1} H_2O). Apparently, post-translational regulatory mechanisms such as reduced Na^+/K^+-ATPase trafficking to and insertion into the septal cell membranes, as well as storage as inactive enzyme in intracellular vesicles (Paller, 1994; McNamara and Torres, 1999; Lovett et al., 2006), also downregulate Na^+/K^+-ATPase activity, awaiting the return of hyposmotic conditions. Such weak anisosmotic extracellular regulation also might be complemented by isosmotic intracellular regulation, as gill and muscle total free amino acids in *M. amazonicum* from the same population increase by 62 and 72%, respectively, after 5 days of acclimation to 25‰ S (Augusto et al., 2007).

V-ATPase activity and B-subunit expression sustain a good proportion of overall ion uptake by *M. amazonicum* gills when in freshwater, and other apical antiporters, such as the Na^+/H^+ exchanger (Towle et al., 1997), might also contribute to Na^+ uptake. Furthermore, the initial increase in V-ATPase mRNA expression could reflect rapid cell volume regulation based on transport of inorganic osmolytes from the extracellular fluid, energized by proton export. By contrast, the marked decrease in V-ATPase B-subunit mRNA expression and V_1-ATPase activity observed on salinity acclimation to levels 4-fold below those found in freshwater (see Fig. 2D) reflect downregulated ion capture mechanisms linked to proton extrusion such as, for example, Na^+ influx driven by the potential difference across the apical membrane, as confirmed by the absence of Bafilomycin A_1 inhibitable activity in gill homogenates after 10 days of salinity exposure. V-ATPase activities have been measured in the anterior and posterior gills of a variety of crabs, including *Eriocheir sinensis* (Onken and Putzenlechner, 1995) and *Dilocarcinus pagei* (Weihrauch et al., 2004). However, the crustacean gill V-ATPase has not been previously characterized kinetically, and the effect of salinity acclimation on V-ATPase activity in palaemonids is unknown. Compared with V-ATPases from mouse kidney (Sun-Wada et al., 2005), and from yeast, corn and freshwater clam (Dröse and Altendorf, 1997), the *M. amazonicum* enzyme exhibits lower ATP and Bafilomycin A_1 affinities.

The subcellular location of transport proteins is crucial to the directionality of transport mechanisms. In *M. amazonicum* gills, pillar cells possessing thick, radiating apical flanges separated by an intralamellar septum constitute the lamellar epithelium, forming two symmetrical compartments through which hemolymph flows, which are further subdivided vertically by the pillar cell bodies, maximizing contact. This arrangement is very similar to that seen in *M. olfersi* (Freire and McNamara, 1995; McNamara and Lima, 1997), the differences being restricted to features such as the pillar cell flanges, which are three times thicker in *M. amazonicum*, for example. The apical surface of the lamellar epithelium in both *M. amazonicum* and *M. olfersi* (McNamara and Lima, 1997) is highly amplified by extensive evaginations associated with mitochondria in the sub-apical cytoplasm, evidently coupled to ion capture. Such evaginations would increase the apical membrane area available for the insertion of transport proteins such as the V-ATPase and the HCO_3^-/Cl^- exchanger. The striking decrease in V-ATPase activity seen during salinity acclimation in *M. amazonicum* derives from decreased expression of the V-ATPase B-subunit mRNA and is likely accompanied by a reduction in the number and length of the apical evaginations, and in the thickness of the pillar cell flanges, such as is seen in *M. olfersi* (McNamara and Lima, 1997), that presumably house this ATPase. In *E. sinensis*, Cl^- transport *via* the HCO_3^-/Cl^- exchanger is HCO_3^- gradient-dependent and is sustained by a V-ATPase putatively located in the apical pillar cell evaginations (Onken, 1996). Zare and Greenaway (Zare and Greenaway, 1998) propose that a V-ATPase actively energizes gill Na^+ uptake in the freshwater crayfish *Cherax destructor*, a model that is now considered to be generally applicable to freshwater organisms (see Kirschner, 2004; Freire et al., 2008a). These two mechanisms of Cl^- (Onken, 1996) and Na^+ uptake (Lin and Randall, 1993; Zare and Greenaway, 1998; Weihrauch et al., 2001) across a highly energized interface, sustained by the numerous mitochondria in the apical pillar cell cytoplasm, might effect the first step of salt uptake in freshwater palaemonids such as *M. amazonicum*.

The intralamellar septal cells also exhibit a conspicuously augmented membrane system: deep invaginations of the plasmalemma in contact with the hemolymph. These are also associated with numerous mitochondria and characterize a typical crustacean ion-transporting epithelium, much like those seen in brachyurans (Towle and Kays, 1986; Taylor and Taylor, 1992; Péqueux, 1995). In *M. olfersi*, such invaginations house the Na^+/K^+-ATPase also present in the specialized junctions formed with the abutting pillar cell bodies (McNamara and Torres, 1999); this interface is characterized by abundant, finely granular material in the extracellular space and is characteristic of the palaemonid gill epithelium. Clearly both Na^+ uptake from freshwater and, particularly, Cl^- secretion in saline media *via* the apical pillar cell evaginations rely on cellular machinery involving various ion transporters that are dependent on the electrochemical gradient furnished by the Na^+/K^+-ATPase located in the septal cell invaginations.

ACKNOWLEDGEMENTS

This investigation constitutes part of an MSc dissertation submitted by R.O.F. to the Postgraduate Program in Comparative Biology, Department of Biology, FFCLRP, Universidade de São Paulo (USP). We thank Dr Zilá L. P. Simões (Laboratório de Biologia e Genética do Desenvolvimento), FFCLRP, USP, for access to molecular biology facilities, Nara M. Belli for performing the V-ATPase assays, Dr Andrea C. Quiapim for DNA sequencing and Susie Teixeira Keiko for technical support. Research was financed by grants from the Fundação de Amparo à Pesquisa do Estado de São Paulo (FAPESP #2007/04870-9 to J.C.M. and #2008/57830-7 to R.P.M.F.) and the Conselho Nacional de Desenvolvimento Científico e Tecnológico (CNPq #304174-2006-8 to J.C.M. and #471933/2008-2 to R.P.M.F.), and the Coordenadoria de Aperfeiçoamento de Pessoal de Nível Superior (CAPES), from whom R.O.F. received an MSc scholarship (2005-2007). J.C.M. and R.P.M.F. received research scholarships from CNPq. Shrimp were collected under IBAMA permit #070/2004 issued by the Instituto Brasileiro do Meio Ambiente e dos Recursos Naturais Renováveis. We are most grateful to Dr Dirk Weihrauch for kindly providing the degenerate NaK_10F/16R and HAT_F2/R4 primers.

REFERENCES

Altschul, S. F., Gish, W., Miller, W., Myers, E. W. and Lipman, D. J. (1990). Basic local alignment search tool. *J. Mol. Biol.* **215**, 403-410.

Anger, K. (1995). The conquest of freshwater and land by marine crabs: adaptations in life-history patterns and larval bioenergetics. *J. Exp. Mar. Biol. Ecol.* **193**, 119-145.

Augusto, A., Greene, L. J., Laure, H. J. and McNamara, J. C. (2007). The ontogeny of isosmotic intracellular regulation in the diadromous, freshwater palaemonid shrimps, *Macrobrachium amazonicum* and *M. olfersi* (Crustacea, Decapoda). *J. Crust. Biol.* **27**, 626-634.

Augusto, A., Pinheiro, A. S., Greene, L. J., Laure, H. J. and McNamara, J. C. (2009). Evolutionary transition of freshwater by ancestral marine palaemonids: evidence from osmoregulation of in a tide pool shrimp. *Aquat. Biol.* **7**, 113-122.

Ausubel, F. M., Brent, R., Kingston, R. E., Moore, D. D., Seidman, J. G., Smith, J. A. and Struhl, K. (1992). *Current protocols in molecular biology*, pp. 2.1.1–2.4.5. New York: Greene Publishing Associates & Wiley-Interscience.

Belli, N. M., Faleiros, R. O., Firmino, K. C. S., Masui, D. C., Leone, F. A., McNamara, J. C. and Furriel, R. P. M. (2009). Na,K-ATPase activity and epithelial interfaces in gills of the freshwater shrimp *Macrobrachium amazonicum* (Decapoda, Palaemonidae). *Comp. Biochem. Physiol. A Physiol.* **152**, 431-439.

Berger, V. J. and Kharazova, A. D. (1997). Mechanism of salinity adaptation in marine mollusks. *Hydrobiologia* **355**, 115-126.

Bond-Buckup, G. and Buckup, L. (1989). Os Palaemonidae de águas continentais do Brasil meridional (Crustacea, Decapoda). *Rev. Bras. Biol.* **49**, 883-896.

Chung, K. F. and Lin, H. C. (2006). Osmoregulation and Na,K-ATPase expression in osmoregulatory organs of *Scylla paramamosain*. *Comp. Biochem. Physiol. A Physiol.* **144**, 48-57.

Collart, O. and Rabelo, H. (1996). Variation in egg size of the fresh-water prawn *Macrobrachium amazonicum* (Decapoda: Palaemonidae). *J. Crust. Biol.* **16**, 684-688.

Copeland, D. E. (1968). Fine structure of salt and water uptake in the land crab *Gecarcinus lateralis*. *Am. Zool.* **8**, 417-432.

Copeland, D. E. and Fitzjarrell, A. T. (1968). The salt absorbing cells in the gills of the blue crab (*Callinectes sapidus*, Rathbun) with notes on modified mitochondria. *Z. Zellforsch.* **92**, 1-22.

Dröse, S. and Altendorf, K. (1997). Bafilomycins and concanamycins as inhibitors of V-ATPases and P-ATPases. *J. Exp. Biol.* **200**, 1-8.

Evans, D. H., Piermarini, P. M. and Potts, W. T. W. (1999). Ionic transport in the fish gill epithelium. *J. Exp. Zool.* **283**, 641-652.

Freire, C. A. and McNamara, J. C. (1995). Fine structure of the gills of the fresh-water shrimp *Macrobrachium olfersii* (Decapoda): effect of acclimation to high salinity medium and evidence for involvement of the lamellar septum in ion uptake. *J. Crust. Biol.* **15**, 103-116.

Freire, C. A., Cavassin, F., Rodrigues, E. M., Torres, A. H. and McNamara, J. C. (2003). Adaptive patterns of osmotic and ionic regulation, and the invasion of fresh water by the palaemonid shrimps. *Comp. Biochem. Physiol. A Physiol.* **136**, 771-778.

Freire, C. A., Onken, H. and McNamara, J. C. (2008a). A structure function analysis of ion transport in crustacean gills and excretory organs. *Comp. Biochem. Physiol. A Physiol.* **51**, 272-304.

Freire, C. A., Amado, E. M., Souza, L. R., Veiga, M. P., Vitule, J. R., Souza, M. M. and Prodocimo, V. (2008b). Muscle water control in crustaceans and fishes as a function of habitat, osmoregulatory capacity, and degree of euryhalinity. *Comp. Biochem. Physiol. A Physiol.* **149**, 435-446.

Furriel, R. P. M., McNamara, J. C. and Leone, F. A. (2000). Characterization of (Na^+, K^+)-ATPase in gill microsomes from the freshwater shrimp *Macrobrachium olfersii*. *Comp. Biochem. Physiol. B Biochem. Mol. Biol.* **126**, 303-315.

Genovese, G., Luchetti, C. G. and Luquet, C. M. (2004). Na^+/K^+-ATPase activity and gill ultrastructure in the hyper-hypo-regulating crab *Chasmagnathus granulatus* acclimated to dilute, normal, and concentrated seawater. *Mar. Biol.* **144**, 111-118.

Gilles, R. and Péqueux, A. (1986). Physiological and ultrastructural studies of NaCl transport in crustacean gills. *Boll. Zool.* **53**, 173-182.

Holthuis, L. B. (1952). A general revision of the Palaemonidae (Crustacea, Decapoda, Natantia) of the Americas. II. The subfamily Palaemoninae. *Occ. Pap. Allan Hancock Found.* **12**, 1-136.

Jalihal, D. R., Sankolli, K. N. and Shenoy, S. (1993). Evolution of larval development patterns and process of freshwaterization in the prawn genus *Macrobrachium* Bate, 1868 (Decapoda, Palaemonidae). *Crustaceana* **65**, 365-376.

Kamemoto, F. I. (1991). Neuroendocrinology of osmoregulation in crabs. *Zool. Sci.* **8**, 827-833.

Kirschner, L. B. (2004). The mechanism of sodium chloride uptake in hyperregulating aquatic animals. *J. Exp. Biol.* **207**, 1439-1452.

Lima, A. G., McNamara, J. C. and Terra, W. R. (1997). Regulation of hemolymph osmolytes and gill Na^+/K^+-ATPase activities during acclimation to saline media in the freshwater shrimp *Macrobrachium olfersii* (Wiegmann, 1836) (Decapoda, Palaemonidae). *J. Exp. Mar. Biol. Ecol.* **215**, 81-91.

Lin, H. and Randall, D. J. (1993). H^+-ATPase activity in crude homogenates of fish gill tissue: inhibitor sensitivity and environmental and hormonal regulation. *J. Exp. Biol.* **180**, 163-174.

Lohrman, D. M. and Kamemoto, F. I. (1987). The effect of dibutyryl cAMP on sodium uptake by isolated perfused gills of *Callinectes sapidus*. *Gen. Comp. Endocrinol.* **65**, 300-305.

Lovett, D. L., Verzi, M. P., Burgents, J. E., Tanner, C. A., Glosmski, K., Lee, J. J. and Towle, D. W. (2006). Expression profiles of Na,K-ATPase during acute and chronic hypo-osmotic stress in the blue crab *Callinectes sapidus*. *Biol. Bull.* **211**, 58-65.

Lowy, R. J., Dawson, D. C. and Ernst, S. A. (1989). Mechanism of ion transport by avian salt gland primary cell cultures. *Am. J. Physiol.* **256**, 1184-1191.

Lucu, C. and Flik, G. (1999). Na^+-K^+-ATPase and Na^+/ Ca^{2+} exchange activities in gills of hyperregulating *Carcinus maenas*. *Am. J. Physiol.* **276**, 490-499.

Lucu, C. and Towle, D. W. (2003). Na^+,K^+-ATPase in gills of aquatic crustacea. *Comp. Biochem. Physiol. A Physiol.* **135**, 195-214.

Luquet, C. M., Pellerano, G. and Rosa, G. (1997). Salinity-induced changes in the fine structure of the gills of the semiterrestrial estuarine crab *Uca uruguayensis*. *Tissue Cell* **29**, 495-501.

Luquet, C. M., Genovese, G., Rosa, G. A. and Pellerano, G. N. (2002). Ultrastructural changes in the gill epithelium of the crab *Chasmagnathus granulatus* (Decapoda: Grapsidae) in diluted and concentrated seawater. *Mar. Biol.* **141**, 753-760.

Luquet, C. M., Weihrauch, D., Senek, M. and Towle, D. W. (2005). Induction of branchial ion transporter mRNA expression during acclimation to salinity change in the euryhaline crab *Chasmagnathus granulatus*. *J. Exp. Biol.* **208**, 3627-3636.

Martinez, C. B., Harris, R. R. and Santos, M. C. (1998). Transepithelial potential differences and sodium fluxes in isolated perfused gills of the mangrove crab (*Ucides cordatus*). *Comp. Biochem. Physiol. A Physiol.* **120**, 227-236.

Masui, D. C., Furriel, R. P. M., McNamara, J. C., Mantelatto, F. L. M. and Leone, F. A. (2002). Modulation by ammonium ions of gill microsomal (Na^+,K^+)-ATPase in the swimming crab *Callinectes danae*: a possible mechanism for regulation of ammonia excretion. *Comp. Biochem. Physiol. C Pharmacol. Toxicol. Endocrinol.* **132**, 471-482.

McNamara, J. C. and Lima, A. G. (1997). The route of ion water movements across the gill epithelium of the freshwater shrimp *Macrobrachium olfersii* (Decapoda, Palaemonidae): evidence from ultrastructural changes induced by acclimation to saline media. *Biol. Bull.* **192**, 321-331.

McNamara, J. C. and Torres, A. H. (1999). Ultracytochemical location of Na^+/K^+-ATPase activity and effects of high salinity acclimation in gill and renal epithelia of the freshwater shrimp *Macrobrachium olfersii* (Crustacea, Decapoda). *J. Exp. Zool.* **284**, 617-628.

McNamara, J. C., Moreira, G. S. and Moreira, P. S. (1983). The effects of salinity on respiratory metabolism, survival and moulting in the first zoea of *Macrobrachium amazonicum* (Heller) (Crustacea, Palaemonidae). *Hydrobiologia* **101**, 239-242.

Mendonça, N. N., Masui, D. C., McNamara, J. C., Leone, F. A. and Furriel, R. P. M. (2007). Long-term exposure of the freshwater shrimp *Macrobrachium olfersi* to elevated salinity: effects on gill (Na^+,K^+)-ATPase α-subunit expression and K^+-phosphatase activity. *Comp. Biochem. Physiol. A Physiol.* **146**, 534-543.

Moreira, G. S. and McNamara, J. C. (1986). The effect of salinity on the upper thermal limits of survival and metamorphosis during larval development in *Macrobrachium amazonicum* (Heller) (Decapoda, Palaemonidae). *Crustaceana* **50**, 231-238.

Moreira, G. S., McNamara, J. C., Shumway, S. E. and Moreira, P. S. (1983). Osmoregulation and respiratory metabolism in Brazilian *Macrobrachium* (Decapoda, Palaemonidae). *Comp. Biochem. Physiol. A Physiol.* **74**, 57-62.

Mount, D. B., Delpire, E., Gamba, G., Hall, A. E., Poch, E., Hoover, R. S. and Hebert, S. C. (1998). The electroneutral cation-chloride cotransporters. *J. Exp. Biol.* **201**, 2091-2102.

Murphy, N. P. and Austin, C. M. (2005). Phylogenetic relationships of the globally distributed freshwater prawn genus *Macrobrachium* (Crustacea: Decapoda: Palaemonidae): biogeography, taxonomy and the convergent evolution of abbreviated larval development. *Zool. Scripta* **34**, 187-197.

Onken, H. (1996). Active and electrogenic absorption of Na^+ and Cl^- across posterior gills of *Eriocheir sinensis*: influence of short-term osmotic variations. *J. Exp. Biol.* **199**, 901-910.

Onken, H. and Putzenlechner, M. (1995). A V-ATPase drives active, electrogenic and Na^+-independent Cl^- absorption across the gills of *Eriocheir sinensis*. *J. Exp. Biol.* **198**, 767-774.

Onken, H., Tresguerres, M. and Luquet, C. M. (2003). Active NaCl absorption across posterior gills of hyperosmoregulating *Chasmagnathus granulatus*. *J. Exp. Biol.* **206**, 1017-1023.

Paller, M. S. (1994). Lateral mobility of Na,K-ATPase and membrane lipids in renal cells. Importance of cytoskeletal integrity. *J. Membr. Biol.* **142**, 127-135.

Péqueux, A. (1995). Osmotic regulation in crustaceans. *J. Crust. Biol.* **15**, 1-60.

Pereira, G. and Garcia, A. (1995). Larval development of *Macrobrachium reyesi* Pereira (Decapoda: Palaemonidae), with a discussion on the origin of abbreviated development in palaemonids. *J. Crust. Biol.* **15**, 117-133.

Provérbio, T., Zanders, P., Marín, R., Rodríguez, J. M. and Proverbio, F. (1990). Effects of Na^+ and/or K^+ on the Mg^{2+}-dependent ATPase activities in shrimp (*Macrobrachium amazonicum*) gill homogenates. *Comp. Biochem. Physiol. B Biochem. Mol. Biol.* **97**, 383-390.

Read, S. M. and Northcote, D. H. (1981). Minimization of variation in the response to different proteins of the Coomassie blue G dye-binding assay for protein. *Anal. Biochem.* **116**, 53-64.

Reynolds, E. S. (1963). The use of lead citrate at high pH as an electron-opaque stain in electron microscopy. *J. Cell Biol.* **17**, 208-212.

Riestenpatt, S., Zeiske, W. and Onken, H. (1994). Cyclic AMP stimulation of electrogenic uptake of Na^+ and Cl^- across the gill epithelium of the Chinese crab *Eriocheir sinensis*. *J. Exp. Biol.* **188**, 159-174.

Riestenpatt, S., Onken, H. and Siebers, D. (1996). Active absorption of Na^+ and Cl^- across the gill epithelium of the shore crab *Carcinus maenas*: voltage-clamp and ion-flux studies. *J. Exp. Biol.* **199**, 1545-1554.

Riordan, J. R., Forbush, B. and Hanrahan, J. W. (1994). The molecular basis of chloride transport in shark rectal gland. *J. Exp. Biol.* **196**, 405-418.

Sanger, F., Nicklen, S. and Coulson, A. R. (1977). DNA sequencing with chain-terminating inhibitors. *Proc. Natl. Acad. Sci. USA* **74**, 5463-5467.

Santos, F. H. and McNamara, J. C. (1996). Neuroendocrine modulation of osmoregulatory parameters in the freshwater shrimp *Macrobrachium olfersii* (Wiegmann) (Crustacea, Decapoda). *J. Exp. Mar. Biol. Ecol.* **206**, 109-120.

Santos, L. C. F., Belli, N. M., Augusto, A., Masui, D. C., Leone, F. A., McNamara, J. C. and Furriel, R. P. M. (2007). Gill (Na^+,K^+)-ATPase in diadromous, freshwater palaemonid shrimps: species-specific kinetic characteristics and α-subunit expression. *Comp. Biochem. Physiol. A Physiol.* **148**, 178-188.

Schales, O. and Schales, S. S. (1941). A simple and accurate method for the determination of chloride in biological fluids. *J. Biol. Chem.* **140**, 879-883.

Sollaud, M. E. (1923). Le développment larvaire des 'Palaemoninae'. I. Partie descriptive. La condensation progressive de l'ontogénèse. *Bull. Biol. Fr. Belg.* **57**, 509-603.

Sommer, M. J. and Mantel, L. H. (1988). Effect of dopamine, cyclic AMP, and pericardial organs on sodium uptake and Na, K-ATPase activity in gills of the green crab, *Carcinus maenas* (L). *J. Exp. Biol.* **248**, 272-277.

Sommer, M. J. and Mantel, L. H. (1991). Effects of dopamine and acclimation to reduced salinity on the concentration of cyclic AMP in the gills of the green crab, *Carcinus maenas* (L). *Gen. Comp. Endocrinol.* **82**, 364-368.

Sun-Wada, G. H., Tabata, H. and Kawamura, N. (2005). Selective assembly of V-ATPase subunit isoforms in mouse kidney. *J. Bioenerg. Biomembr.* **37**, 415-418.

Taylor, H. H. and Taylor, E. W. (1992). Gills and lungs: the exchange of gases and ions. In *Microscopic Anatomy of Invertebrates,* Vol. 10. *Decapod Crustacea* (ed. W. F. Harrison and A. G. Humes), pp. 203-293. New York: Wiley-Liss, Inc.

Towle, D. W. and Kays, W. T. (1986). Basolateral localization of $Na^+ + K^+$-ATPase in gill epithelium of two osmoregulating crabs, *Callinectes sapidus* and *Carcinus maenas*. *J. Exp. Zool.* **239**, 311-318.

Towle, D. W., Rushton, M. E., Heidysch, D., Magnani, J. J., Rose, M. J., Amstutz, A., Jordan, M. K., Shearer, D. W. and Wu, W. S. (1997). Sodium/proton antiporter in the euryhaline crab *Carcinus maenas*: molecular cloning, expression and tissue distribution. *J. Exp. Biol.* **200**, 1003-1014.

Towle, D. W., Paulsen, R. S., Weihrauch, D., Kordylewski, M., Salvador, C., Lignot, J. H. and Pierrot, C. S. (2001). Na^+/K^+-ATPase in gills of the blue crab *Callinectes sapidus*: cDNA sequencing and salinity-related expression of α-subunit mRNA and protein. *J. Exp. Biol.* **204**, 4005-4012.

Weihrauch, D., Ziegler, A., Siebers, D. and Towle, D. W. (2001). Molecular characterization of V-type H^+-ATPase (b-subunit) in gills of euryhaline crabs and its physiological role in osmoregulatory ion uptake. *J. Exp. Biol.* **204**, 25-37.

Weihrauch, D., McNamara, J. C., Towle, D. W. and Onken, H. (2004). Ion-motive ATPases and active, transbranchial NaCl uptake in the red freshwater crab, *Dilocarcinus pagei* (Decapoda, Trichodactylidae). *J. Exp. Biol.* **207**, 4623-4631.

Zanders, P. and Rodríguez, J. M. (1992). Effects of temperature and salinity stress on osmoionic regulation in adults and on oxygen consumption in larvae and adults of *Macrobrachium amazonicum* (Decapoda, Palaemonidae). *Comp. Biochem. Physiol. A Physiol.* **101**, 505-509.

Zare, S. and Greenaway, P. (1998). The effects of moulting and sodium depletion on sodium transport and activities of Na^+/K^+-ATPase, and V-ATPase in the freshwater crayfish *Cherax destructor* (Crustacea: Parastacidae). *Comp. Biochem. Physiol. A Physiol.* **119**, 739-745.

Zatta, P. (1987). Dopamine, noradrenaline and serotonin during hypoosmotic stress of *Carcinus maenas*. *Comp. Biochem. Physiol. A Physiol.* **96**, 479-481.